Building and Environment 242 (2023) 110580

Contents lists available at ScienceDirect

Building and Environment

journal homepage: www.elsevier.com/locate/buildenv

Seasonal impacts of built environment and its interactions on urban park cooling effects in Nanjing, China

Zhengyuan Liang [a], Zhiming Li [a,*], Zhengxi Fan [b]

[a] College of Landscape Architecture, Nanjing Forestry University, Nanjing, Jiangsu Province, 210037, China
[b] School of Architecture, Southeast University, Nanjing, Jiangsu Province, 210096, China

ARTICLE INFO

Keywords:
Urban parks
Seasonal cooling effects
Built environment
Interactions
Geographic detector
Nanjing central districts

ABSTRACT

Urban parks offer a nature-based solution to mitigate urban heat islands (UHIs). Although the urban park cooling effect (UPCE) has been extensively investigated, the assessment of its seasonal variation remains uncertain, which hinders optimization. Taking 217 parks in Nanjing central districts as samples, this study calculated the urban park cooling magnitude (UPCM) of four seasons and used the turning point method (TPM) to characterize the multidimensional characteristics of the urban park seasonal cooling effect (UPSCE). Using models such as geographic detectors and multiple stepwise regression, we determined the impacts of built environment and its interactions on the UPSCE. According to the results, urban parks demonstrated the best cooling in summer, at 1.28 °C on average, which was higher than that in spring (1.07 °C) and autumn (1.01 °C) and almost four times that in winter (0.30 °C). The UPCE is greatly affected by factors such as the park area, park perimeter (PP), landscape shape index, normalized difference vegetation index (NDVI), normalized difference water index (NDWI), elevation, and surrounding building density, which vary with seasons. Among them, the NDVI, NDWI, and PP proved to be the dominant factors, explaining 55.7%, 53.3%, 62.0%, and 50.5%, respectively, of the variance of UPCM in the four seasons. In addition, the interactions of built environment will significantly enhance the UPCE, and the intensity differ with seasons. These findings will support the development of more sustainable urban microclimate policies and improve the surface thermal environment and thermal comfort of urban parks and their surroundings in different seasons.

1. Introduction

Urban heat islands (UHIs) occur when urban areas are hotter than their rural or natural neighbors due to excessive impervious surfaces, heat-trapping materials, and vegetation loss [1–4]. Globally, an increasing number of cities are experiencing frequent, intense, and persistent heat waves, which threaten human physical and mental health, reduce the vitality of urban spaces, and increase energy supply loads [5,6]. Moreover, continuing migration to urban areas increases the number of people exposed to dangerous heat [7]. According to statistics, more than 20,000 people died as a result of heatwaves in each of the years 2013, 2017, and 2019 in China, and thousands die in heatwaves every year in the United States [1,5]. As a thermal intervention, air conditioning reduces the impact on individuals, but greenhouse gases exacerbate the heat island effect, with inequalities in heat-vulnerable communities [8,9]. Hence, more efficient and sustainable alternatives are needed.

Urban parks have proven effective at mitigating UHIs and improving surface thermal environment and usually consist of blue spaces, green spaces, and recreational service facilities [10,11]. Due to the large heat capacity of vegetation transpiration and water bodies, urban parks have better heat exchange, and hence cooling, than surrounding areas [12,13]. Facing summer heat, cities have developed urban blue-green infrastructure (e.g., urban parks, water bodies, green streets, and green roofs) to reduce solar radiation absorption and heat storage capacity, aiming to alleviate UHI effects [14,15], and scholars in the fields of architecture, urban planning, and environmental research are all researching solutions to mitigate UHI effects.

Investigations have demonstrated the UPCE through the temperature difference between park interiors and their surrounding areas. Urban parks are cooler than their surroundings in summer heat, by 1–2 °C and sometimes by 5–7 °C, according to many site-based measurements [16], and the UPCE can be can quantified such as by field measurement [2,17,18], computer numerical simulation [18,19], and buffer zones [12,20].

* Corresponding author.
E-mail addresses: Liangzhengyuan@njfu.edu.cn (Z. Liang), Lizhiming7507@njfu.edu.cn (Z. Li), fanzx0058@seu.edu.cn (Z. Fan).

https://doi.org/10.1016/j.buildenv.2023.110580
Received 7 April 2023; Received in revised form 30 June 2023; Accepted 30 June 2023
Available online 3 July 2023
0360-1323/

As urban-scale thermal data are difficult to obtain, land surface temperature (LST) is viewed as important measures in urban thermal-related studies. Usually, LST is obtained by inversion to earth observation images, such as the Landsat series, which has the advantages of relatively high precision and continuous coverage. According to previous studies, LST is highly correlated with air temperature and thermal comfort, and severe LST can affect residents' thermal comfort and be life-threatening in hot seasons [21,22]. Combined with the moisture index, NDVI, etc., LST has been widely used in the macroscopic dynamic monitoring of UHIs and thermal comfort distribution [9,23,24]. For example, using Landsat-derived thermal comfort data and population datasets, Wu et al. (2023) calculated city-level thermal comfort exposures for 398 cities in the United States from 2000 to 2020. Therefore, on the basis of buffer zones, LST can be effectively used to estimate urban parks' cooling to surrounding surface thermal environment, thereby improving urban microclimate and thermal comfort [25,26].

Urban park cooling to the buffer zone (i.e., the surrounding environment) can be defined by the fixed radius method [27], equal area method [28,29], equal radius method (ERM) [30,31], turning point method (TPM) [32–34]. Liao (2021) and Xiao (2023) compared the five methods and recommended the ERM and TPM to quantify the UPCE. TPM-maximum perspective and TPM-cumulation perspective respectively consider the maximum and spatial continuous effects, and some indicators have been selected, such as the park cooling area, cooling distance, cooling efficiency [35–37], cooling intensity, and cooling gradient [14,32]. Indicators represent different cooling characteristics, and measurement results can vary. Hence, the quantification of the UPCE has not been conclusive [28,38], and it requires multiple dimensions to provide more comprehensive insights to select the most appropriate natural interventions.

Determining built environment factors of the UPCE in summer heat is important to optimize the layout and landscape of urban parks to improve their cooling capability. These factors include the park area, perimeter, shape index, land cover type, NDVI, and NDWI, which measure the blue-green space [4,10,27–31,34,39]. Exploring the UPCE and its built environment factors based on specific technical models often has gaps in factor importance. Although the landscape shape index varies in practice in different cities [40,41], the park area, perimeter, and blue-green space indexes have all been shown to positively affect the UPCE [12,27,30]. A few studies have more deeply investigated the impact of internal park landscape factors, such as the landscape percentage (PLAND), largest patch index, aggregation index (AI), and other indicators [42–44]. Xu et al. determined that PLAND and AI explained approximately 54% of the variance in the UPCE. However, the UPCE is influenced not only by its internal microclimate, but also by the surrounding environment [35,45]. A study in Beijing, China, confirmed the nonlinear impacts of surrounding 2D/3D landscapes on the UPCE in heat extremes and normal weather, where the parameters of surrounding buildings (including building density, building height, sky view factor, and frontal area index) and vegetation are the most important indicators [35].

Although the built environment factors affecting the UPCE are becoming more mature, some local factors such as the city center, mountains, and large water systems may also affect the cooling effects of nearby urban parks and must be further explored in combination with the local natural environment. Many studies have examined the individual effects of factors on the UPCE using regression models (e.g., multiple regression [38,46], decision tree regression [34,35], and structural equation modeling [47]) or correlation analysis [28,32,48], but the interactions between factors remains uncertain, which hinders the optimization of UPCE. A geographical detector based on spatially stratified heterogeneity can be used to reach the target [49]. It is not affected by multi-collinearity between variables. Although collinearity may exist between variables, it will not affect the results because each factor is entered separately to explain the dependent variable. Detecting spatial variance through geographic detectors can not only determine the explanatory power of each factor but can also explore the interaction of two factors on dependent variables [49–51], which can effectively explain the complex mechanism of UPCE.

Many scholars believe that frequent and continuous summer heat requires urban parks to exert the maximum cooling effects to improve environment thermal comfort [27,32,33,35]. As a result, studies on urban park cooling effects tend to focus on summer or heat extremes [35,48]. Globally, climate distribution between cities or regions differs greatly. According to the Building Climate Zoning Standard (GB 50178–93) [62], China can be roughly divided into seven zones including severe cold areas, cold areas, hot summer and warm winter, etc. Different zones have distinctive seasonal characteristics [52]. Do urban parks have a strong cooling effect in other seasons except in the hot seasons? Does maximizing UPCE only in hot seasons affect surface thermal environment and thermal comfort in other seasons? Previous studies ignored the UPCE in cold seasons, because in the traditional cognition, urban parks in cold seasons have no cooling effects. To maximize UPCE during the hot seasons, urban planners and environmentalists have proposed a series of cooling optimization schemes [32,33]. In fact, UPCE between different seasons may be synergistic or different, especially in areas with large seasonal contrasts. Therefore, the optimization of UPCE cannot be viewed in isolation of a season, the more important work is to maximize the UPCE in the hot season while avoiding or minimizing negative impacts on thermal comfort in other seasons, like cold seasons. Das et al. (2023) recognized this limitation and affirmed the need for research on UPSCE [48,53].

Over the past 40 years, Nanjing, a megacity in Eastern China, has experienced massive and rapid urban expansion and economic growth, which has resulted in severe heat stress and a high risk of population exposure to summer heat [38]. In summer, maximizing the UPCE is of great significance to improve the urban thermal environment. Nanjing is typical of the many cities in this region of hot summers and cold winters, where the temperature in summers can exceed 40 °C and that in winters can be below −10 °C. Due to the relatively high air humidity in southern cities, damp and cold will significantly increase the discomfort of outdoor activities. Therefore, only considering the maximum of UPCE in summer, when UPCE in winter is still obvious, will affect the thermal comfort of residents using parks. It is necessary to investigate the UPCE and its built environment factors from a broader background, such as seasons and climate zones.

So, the focus of this paper is the seasonal variations of UPCE and how the built environment and its interactions affect these variations. Unlike Xiao et al. (2023) who compared five buffer-based assessment methods of the UPCE to determine the best one, our study focuses closely on "seasonal differences". In addition, another difference is that we believe that UPCE is probably not only a simple superposition of the impact of each built environment factor, but also the result of their interactions. So, they are studies that establish two different research perspectives, using different methods and datasets. This study mainly includes two-aspect works (Fig. 1): First, for quantifying UPSCE, Xiao et al. (2023) compared five commonly used methods based on LST and buffers, we only used the TPM method. According to this method, we used UPCM as the main measure of UPSCE, and defined multidimensional indicators based on previous studies and our understandings. Secondly, we detected impacts of the built environment and its interactions on UPSCE. Using geographic detectors, the individual and interactional impacts of the built environment on UPSCE could be well determined by calculating and comparing single-factor q-values and interactional q-values. In addition, as a supplement, we also used regression analysis to measure dominant factors, and used Pearson heatmap to visualize factor correlations under multidimensional index system.

Taking Nanjing central districts as an example, this study uses larger datasets, including 217 parks and multi-period LSTs of different seasons. More samples and data can draw more general and convincing conclusions. This study aims to determine: (1) how the UPCE varies in different

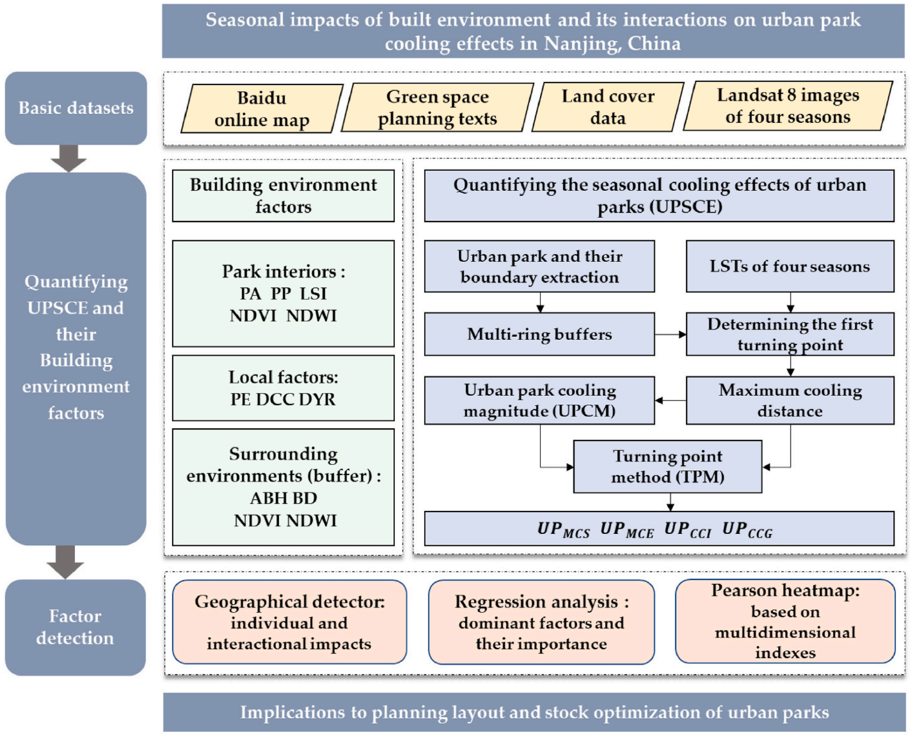

Fig. 1. Methodological framework of this study.

seasons; (2) how built environment and its interactions affect the UPCE in different seasons; and (3) how to maximize the UPCE in hot seasons without compromising land surface thermal environment and thermal comfort in other seasons.

2. Materials and methods

2.1. Study area

Nanjing, located at 31°14′–32°36′N, 118°22′–119°14′E, is a megacity in eastern China, which lies in the subtropical monsoon climate zone, with four distinct seasons, and an annual average temperature of

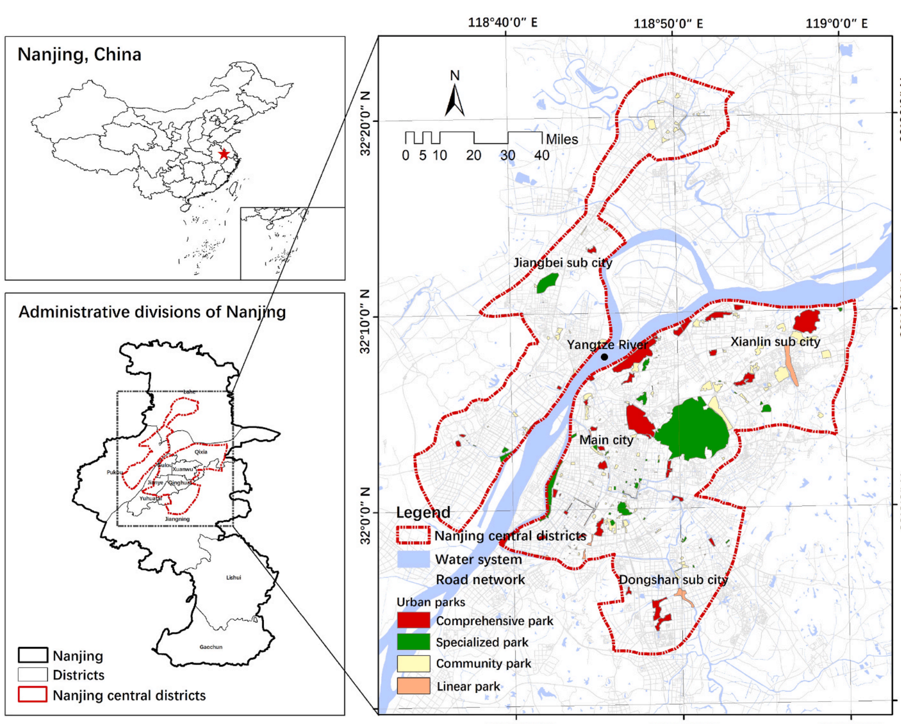

Fig. 2. Locations of 217 urban parks in Nanjing central districts.

15.4 °C. According to the Nanjing Master Planning (2011–2020), at the end of the planning period, it had a total area of 6582 km^2 and a resident population of 10600000 [54].

2.2. Data sources and preprocessing

In 2019, the Nanjing Green and Garden Bureau announced the Nanjing Green Space System Planning (2013–2020) [55], and the government launched a series of urban greening construction projects. The per capita park area in Nanjing has reached 16.18 m^2. This study focuses on 217 parks in Nanjing central districts, which vary by size and type (Fig. 2). The park polygon data were crawled from the open platform of the Baidu online map (https://lbsyun.baidu.com/) and were checked and supplemented according to the Nanjing Green Space System Planning (2013–2020). Green spaces along urban streets are difficult to count accurately due to their small area and fragmented distribution; so, they were excluded.

Other basic data were obtained as follows: (1) the water system and road network data were from the Open Street Map; (2) the land surface temperature (LST) data were obtained by inversion based on a single-window algorithm. In Nanjing, spring, summer, autumn, and fall run respectively from March to May, June to August, September to November, and December to January. This study uses Landsat 8 remote sensing images of four periods in 2021–March 26, August 1, October 4, and December 7—all with cloud cover of less than 2% in Nanjing central districts. These data can be obtained from the geospatial data cloud website (http://www.gscloud.cn/search) and can more typically represent the LST of four seasons in Nanjing. Fig. 3 shows the LST distribution on October 4 in autumn, with the LST range 32.93°C-57.78 °C. The LSTs of the other three seasons are 9.65°C-39.10 °C (March 26), 16.65°C-42.80 °C (October 4), and −7.50 °C–23.12 °C (December 7). The resolution of all LSTs is 30-m.

(3) The building data were crawled on the open platform of the Baidu online map (https://lbsyun.baidu.com/), including information such as building areas and heights.

The resolution of building data is 3-m. Since buildings in the Nanjing central districts are very dense and difficult to visualize clearly, the density (Fig. 4a) and average height (Fig. 4b) of buildings were calculated in units of communities.

2.3. Methodology

2.3.1. Multidimensional measuring method of UPSCE

A park provides cooling services for urban areas in two ways: first, by lowering the temperature within it, thereby providing a place of refuge from the heat, and second, by cooling the area surrounding it. The UPCE on its surrounding built-up areas is spatially continuous. Urban parks are equivalent to cooling islands in the city. The LST gradually increases with the distance from the park edge, but the rate of increase decreases continuously until it becomes zero. In most cases, the effective cooling distance of urban parks to surrounding built-up areas generally does not exceed 900 m [32]. Therefore, we created a multi-ring buffer zone with a basic unit of 30 m for 217 parks in Nanjing central districts (the image resolution of Landsat 8 is 30 m). We drew scatter plots and smooth lines by calculating the average LST within a park and of the built-up land (excluding other blue-green patches) within each buffer circle. When the LST reaches the first turning point (the increase rate is zero), the maximum cooling distance is reached. In this paper, we define the first turning point as L_{FTP} and the park boundary as L_0. (Fig. 5). According to these cooling characteristics and previous studies, we propose a multi-dimensional measurement method for UPSCE based on UPCM and TPM.

2.3.1.1. Urban park cooling magnitude (UPCM). In this paper, UPCM is defined as the difference between the mean LST within the park and the LST at the first turning point. It was used to measure the maximum LST difference between park interiors and non-cooling areas. Its expression is:

$$UPCM = \Delta LST_{max} = |LST_{park} - LST_{FTP}|, \tag{1}$$

where LST_{park} is the mean LST inside a park, and LST_{FTP} is the LST of the first turning point.

2.3.1.2. Multi-dimensional measurement of urban park cooling based on TPM. A park's cooling effect can differ depending on the measurement

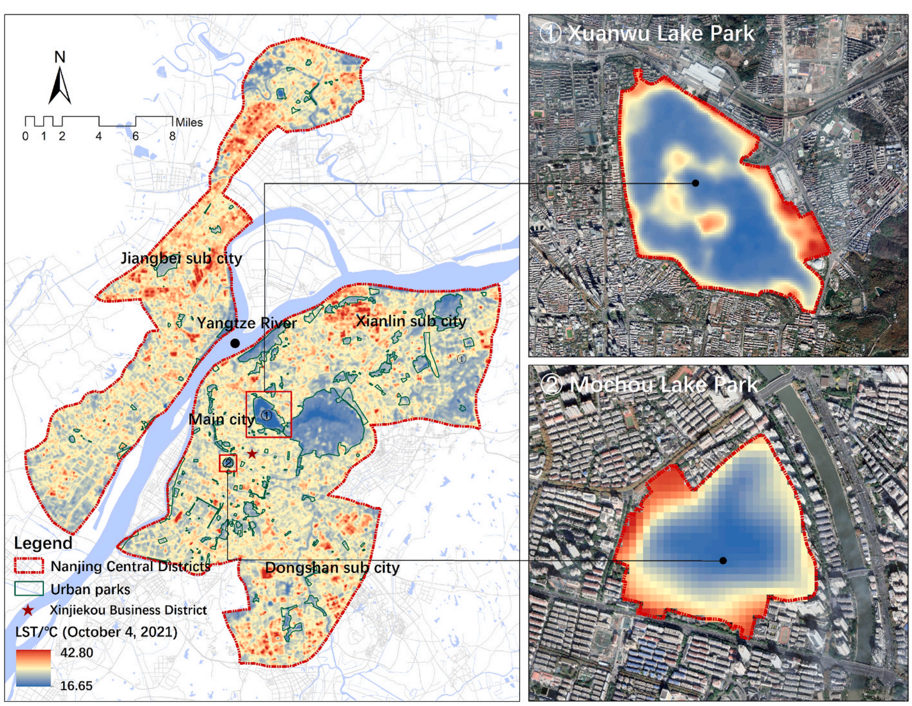

Fig. 3. LST distribution on October 4, 2021.

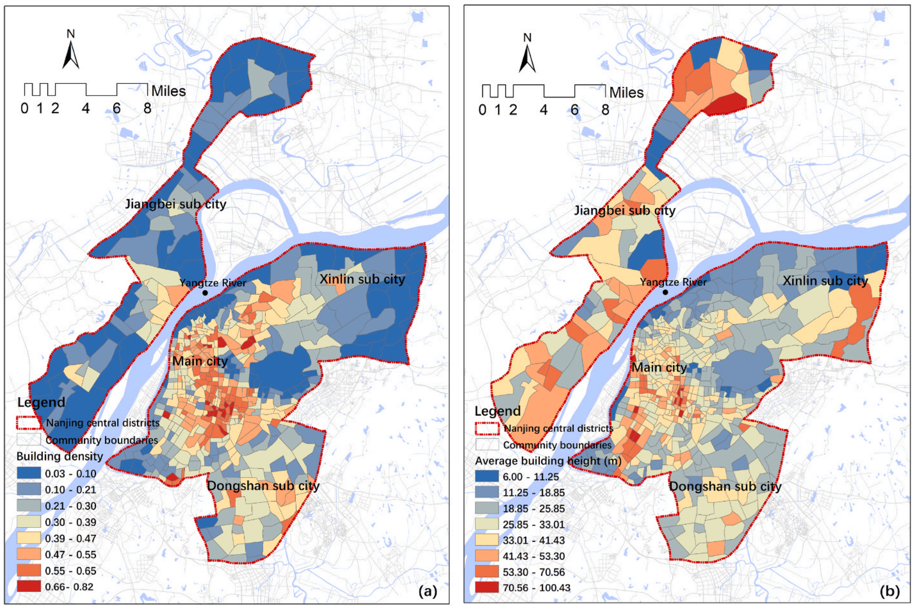

Fig. 4. Distribution of (a) building density and (b) average building height.

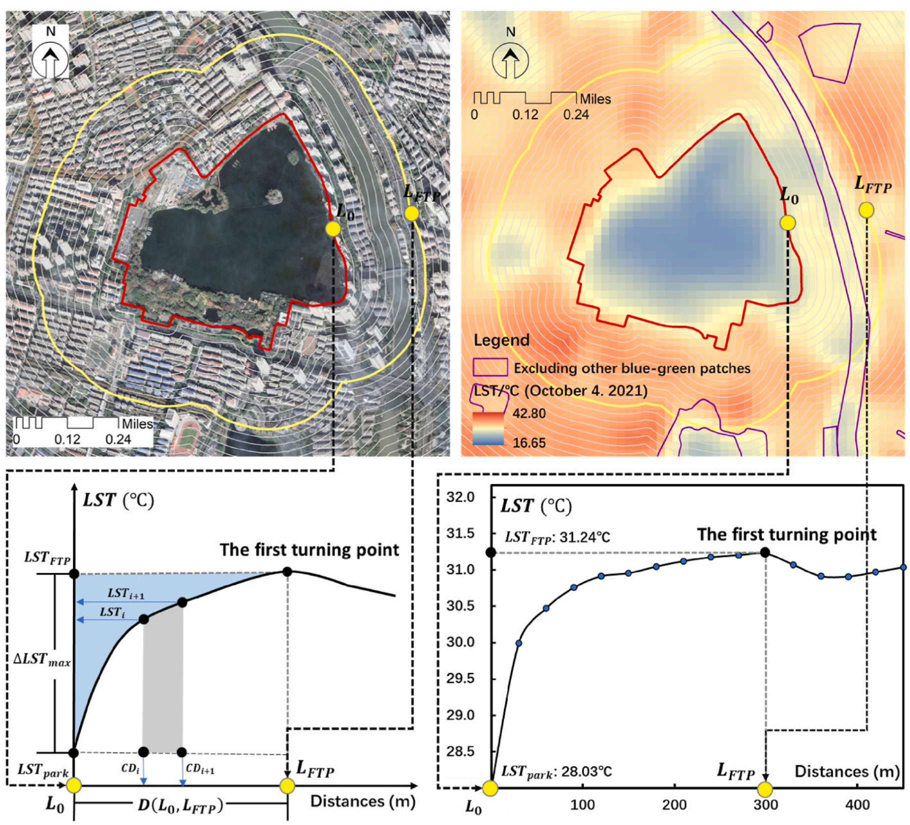

Fig. 5. Schematic diagram of urban park cooling, taking Macho Lake Park as an example.

perspective. Although UPCM can better measure the cooling capacity of urban parks compared with that of general urban areas, it has some limitations in characterizing the UPCE on the surroundings. TPM can be used as a supplement to UPCM in order to reduce possible uncertainties. TPM is one of the commonly used methods to quantify the UPCE. TPM-maximum perspective and TPM-cumulative perspective are two main perspectives for measuring UPCE. Previous studies have defined different indicators based on different viewpoints [27,28,32,39]. In this paper, we develop four indicators: maximum cooling size (UP_{MCS}), maximum cooling efficiency (UP_{MCE}), cumulative cooling intensity (UP_{CCI}), and cumulative cooling gradient (UP_{CCG}). Among them, the first two indicators reflect UPCE from a whole view, and the latter two consider the spatial distribution and distance attenuation of cooling intensity. The specific definitions and expressions are as follows: UP_{MCS} is the maximum area that can be cooled within the maximum cooling distance, i.e.,

$$UP_{MCS} = \sum_{i \in (L_0, L_{FTP})}^{I} Area_{C_i}, \tag{2}$$

and UP_{MCE} is the ratio of the maximum cooling area to the park area, i.e.,

$$UP_{MCE} = \frac{\sum_{i \in (L_0, L_{FTP})}^{I} Area_{C_i}}{PA}, \tag{3}$$

A larger UP_{MCE} indicates a better cooling effect per unit park area. Taking 30 m as the basic unit, where $Area_{C_i}$ is the area of the buffer circle i, I is the total number of buffer circles when the first turning point is reached, and PA is the area of the park itself.

UP_{CCI} is the cumulative cooling intensity along the cooling distance compared to non-cooling areas, i.e.,

$$UP_{CCI} = UPCM * D(L_0, L_{FTP}) - \frac{1}{2} \sum_{i \in (L_0, L_{FTP})}^{I} \left(LST_{i+1} + LST_i - 2LST_{L_0}\right) * (CD_{i+1} - CD_i), \tag{4}$$

and UP_{CCG} is the average cooling intensity, i.e.,

$$UP_{CCG} = \frac{UPCM * D(L_0, L_{FTP}) - \frac{1}{2} \sum_{i \in (L_0, L_{FTP})}^{I} \left(LST_{i+1} + LST_i - 2LST_{L_0}\right) * (CD_{i+1} - CD_i)}{L_{FTP}}. \tag{5}$$

where $D(L_0, L_{FTP})$ is the maximum cooling distance; L_0 is the park boundary; L_{FTP} is the first turning point; LST_i is the average LST of circle i; and CD_i is the distance from circle i to the park boundary.

2.3.2. Built environment influencing UPSCE

The built environment refers to the artificial environment provided for human activities, usually including buildings, squares, landscapes and crowds [56]. Due to the large scale explored in this study, we mainly consider the impact of macro-physical environment factors on UPSCE. They mainly include three types: park internal factors, local factors, and surrounding environment factors, which are not limited to 2D or 3D environmental characteristics. The measurement methods and their reference sources of 12 selected factors are shown in Table 1. It should be pointed out that there are many large and small mountains in Nanjing central districts, including Zijin Mountain, Yuhua Terrace, etc. Which are usually combined with urban parks. Therefore, we considered elevation's impact on UPSCE. The Yangtze River, as the largest river in China, spans the Nanjing central districts. Many studies have proved the cooling effect of water bodies. Hence, we consider the potential impact of distance from the Yangtze River on the UPCE. In addition, the city center is more densely populated than other urban built areas and tends to have a higher LST; so, the distance between the park and the city center (Nanjing Xinjiekou business district) is also taken into account.

2.3.3. Geographical detector

Geographical detectors are spatial statistical models that uncover the driving forces of spatial heterogeneity. They are used to detect the spatial variation of Y; and to detect the extent to which a certain factor X explains the spatial variation of attribute Y. The four types include factor, interaction, ecological, and risk detectors [63]. We used the first two.

2.3.3.1. Factor detector.

The factor detector detects how well the factors X_n explain the park cooling effects Y, as measured by the q value,

$$q = 1 - \frac{\sum_{h=1}^{L} N_h \sigma_h^2}{N\sigma^2} = 1 - \frac{SSW}{SST}, \tag{5a}$$

where h = 1 …, L is the stratification of Y or factor X; N_h and N are the

Table 1
Building environment Factors affecting UPCE.

	Factor	Abbreviation	Formula	Description
Park internal factors	Area (X1) [18,32]	PA	$PA > 0$	–
	Perimeter (X2) [35]	PP	$PP > 0$	–
	Landscape shape index (X3) [34,57]	P_LSI	$P\_LSI = \frac{PP}{2\sqrt{\pi * PA}}, P\_LSI \geq 1$	PA: park area; PP: park perimeter
	Normalized difference vegetation index (X4) [48,58]	P_NDVI	$P\_NDVI = \frac{NIR - Red}{NIR + Red}, 0 \leq P\_NDVI \leq 1$	NIR and Red: reflected radiance values in the near-infrared and red bands, respectively
	Normalized difference water index (X5) [16,59]	P_NDWI	$P\_NDWI = \frac{Green - NIR}{Green + NIR}, 0 \leq P\_NDWI \leq 1$	Green and MIR: reflected radiance values in the green and mid-infrared bands, respectively, of the image
Local factors	Elevation (X6)	PE	$PE \geq 0$	–
	Distance from city center (X7)	P_DCC	$P\_DCC \geq 0$	Shortest straight-line distance to Xinjiekou business district
	Distance from the Yangtze River (X8)	P_DYR	$P\_DYR \geq 0$	Shortest straight-line distance to the Yangtze River
Surrounding environment factors (Buffer zone)	Average building height (X9) [35,60]	B_ABH	$B\_ABH = \frac{\sum_{i=1}^{N} BH_i}{N}, B\_ABH \geq 0$	Average building height in park cooling zone
	Building density (X10) [61,62]	B_BD	$B\_BD = \frac{Area_{bba}}{Area_{pc}}, B\_BD \geq 0$	$Area_{bba}$: total building base area in park cooling zone; $Area_{pc}$: area of park cooling zone
	Normalized difference vegetation index (X11) [39,58]	B_NDVI	$B\_NDVI = \frac{NIR - Red}{NIR + Red}, 0 \leq B\_NDVI \leq 1$	NIR and Red: reflected radiance values in the near-infrared and red bands, respectively
	Normalized difference water index (X12) [16,33]	B_NDWI	$B\_NDWI = \frac{Green - NIR}{Green + NIR}, 0 \leq B\_NDWI \leq 1$	Green and MIR: reflected radiance values in the green and mid-infrared bands, respectively, of the image

numbers of units in stratum h and the global region, respectively; σ_h^2 and σ^2 are the respective variances of the Y values of h and the global region; and SSW and SST are respectively the within and total sum of squares. The q value ranges from 0 to 1, if the stratification is generated by the independent variable X, the larger the value of q, the stronger the explanatory power of the independent variable X to the attribute Y, and vice versa. In extreme cases, a q value of 1 indicates that factor X completely controls the spatial distribution of Y, a q value of 0 indicates that factor X has no relationship with Y, and a q value indicates that X explains 100 × q% of Y [63,64].

2.3.3.2. Interaction detector. The interaction detector detects whether X1 and X2 acting together increase or decrease the explanatory power of Y, or whether their impacts are independent of each other. By calculating and comparing the q value of each single factor and the q value after the superposition of two factors, the geographic detector can detect whether there is an interaction between the two factors, as well as the strength, direction, linearity or nonlinearity of its interaction. The superposition of two factors includes both the multiplication relationship and other relationships, as long as there is a relationship, it can be tested. There are five types of interaction [50,51,64] (Table 2).

Table 2
Two-factor interaction types and relationships.

Description	Interaction type
q (x1∩x2) < Min (q (x1), q (x2))	Weakened, nonlinear
Min (q (x1), q (x2)) < q (x1∩x2) < Max (q (x1), q (x2))	Weakened, unique
q (x1∩x2) > Max (q (x1), q (x2))	Enhanced, bilinear
q (x1∩x2) = q (x1) + q (x2)	Independent
q (x1∩x2) > q (x1) + q (x2)	Enhanced, nonlinear

3. Results

3.1. Seasonal cooling effects of urban parks

3.1.1. Distribution of UPCM of four seasons

Although a sample of 217 parks was used for the study, not all parks have a significant cooling effect, even in summer (Fig. 6). Compared with spring, summer, and autumn, the number of parks with no significant cooling effect in winter was the largest, at 81, and that in summer was the smallest, at 33 (Fig. 7). In summer, there are 53 parks' UPCM reach above 2 °C, the average UPCM reached 1.28 °C, the highest among the seasons, and it was the lowest in winter, at 0.30 °C. The average UPCM of spring and autumn showed little difference. In summer and autumn, the UPCM of the Wulong Mountain Park (4.52 °C and 4.16 °C, respectively) was the largest; in spring, the UPCM of the Xuanwu Lake Park (4.43 °C) was the largest; and in winter, the UPCM of the Grand Theater Park (2.27 °C) was the largest. The UPCMs are similar in spatial distribution in spring, summer, and autumn but not in winter. According to the UPCM measurement, the UPCE are best in summer, followed by that in spring and autumn, and the worst in winter, which is quite different. Each UPCM corresponds to a maximum cooling distance, whose means, in descending order, are summer (125.40 m), autumn (117.93 m), spring (104.38 m), and winter (87.93 m).

3.1.2. Distribution of multidimensional indexes of UPSCE

Although UPCM can characterize the ability of urban parks to reduce LST, multiple perspectives are required to understand their cooling characteristics, especially the UPCE on the surroundings. The mean UP_{MCS} values in spring (0.34 km^2), summer (0.41 km^2), and autumn (0.37 km^2) are much higher than that in winter (0.28 km^2), and the mean UP_{MCS} values in all four seasons are much higher than the median values, especially in winter. This shows that the UP_{MCS} values of most parks are relatively small. Looking at the distribution of UP_{MCS}, larger parks tend to have higher values, and parks with higher UP_{MCE} values tend to be smaller, such as those in main cities (Fig. 8). Fig. 9 further shows the numerical distribution of the multidimensional indexes. In summer, the park effective cooling area for the surrounding area can reach an average of 3.69 times the park area itself, and in winter, the average can reach 2.49 times the size of the park area itself.

The UPCE is evaluated based on UP_{MCS} and UP_{MCE}, which cannot reflect the spatial continuity characteristics. UP_{CCI} and UP_{CCG} are used to address this limitation, respectively reflecting the cumulative intensity and gradient of UPSCE. Among them, the average UP_{CCI} and UP_{CCG} values of parks in summer (73.70 °C • m and 0.43 °C, respectively) are the largest, more than 3 times those in winter (21.20 °C • m and 0.11 °C, respectively), and the mean UP_{CCI} and UP_{CCG} values of parks in spring (54.10 °C • m and 0.35 °C, respectively) and autumn (56.35 °C • m and 0.33 °C, respectively) show little difference. For spatial distribution, the UP_{CCI} and UP_{CCG} values of parks in the main city of Nanjing are greater than those in the three sub-cities.

3.2. Seasonal impacts of built environment and its interactions on UPCE

3.2.1. Statistic analysis of factors

We calculated 12 factors. Since there are many types of deciduous plants in Nanjing, such as ginkgo, beech, and sycamore, we calculated the P_NDVI and B_NDVI in the four seasons, as they varied greatly with the seasons. The statistics of these and other factors are shown in Table 3.

3.2.2. Individual and interactional impacts of factors on UPCM

The factor detector was used to determine how 12 factors contributed to the UPCM. After a preliminary Pearson correlation analysis, it was concluded that the P_DCC, B_ABH, and B_BD would have negative impacts on UPCM. Therefore, before running the geographic detector, we transformed these factors into reciprocals for operation. As shown in Table 4, in spring, PA, PP, P_NDVI, P_NDWI, PE, B_NDVI, and B_BD all have driving effects on UPCM at different significance levels, with PA and PP being the most important, followed by P_NDVI, PE, and B_NDVI. In summer, all factors have significant driving effects on UPCM, except P_LSI and B_NDWI, which are weaker. Compared with spring, the driving effects of P_NDVI, B_NDVI, and B_BD were significantly enhanced, and the driving effects of P_DCC and P_DYR changed from insignificant to significant. In autumn, UPCM was significantly influenced by PA, PP, and P_NDVI, followed by P_NDWI and B_BD, while the remaining factors had little impact. Due to the deciduous trees in non-park areas such as city squares and roads, the driving effects of B_NDVI on UPCM were significantly weakened. In winter, withering green vegetation reduces vegetation coverage, and hence, P_NDVI cannot affect UPCM as significantly as PA, PP, P_NDWI, and P_DCC. It should be noted that P_LSI did not appear to have an extremely significant driving effect on UPCM in any season.

The interaction detector was used to determine whether pairwise interactions between 12 factors would enhance UPCM; further, 55 pairwise interactions were detected for each season, which significantly improved the explanatory power of UPCM, mainly manifested by bilinear enhancement (EB) and nonlinear enhancement (EN). In Fig. 10, the larger the value, the redder the color, indicating a stronger explanatory power for UPCM. Among them, the interaction between PA and PB is an EB in spring and summer, and the other enhancements are nonlinear. In summer and autumn, we find the interaction of P_NDVI and P_NDWI significantly enhanced the explanatory power of UPCM (q = 0.86, q = 0.92, respectively), greater than that in spring and winter (q = 0.70, q = 0.73, respectively). Although some factors, such as P_LSI and B_ABH, have weak impacts on UPCM alone, they can significantly enhance its explanatory power when they interact with other factors. As shown in Fig. 11, we further plot the top 10 pairwise interactions according to the q-values of each season and calculate how much explanatory power is enhanced by the two-factor interaction comparing to the individual cumulations. In summer, the interaction between

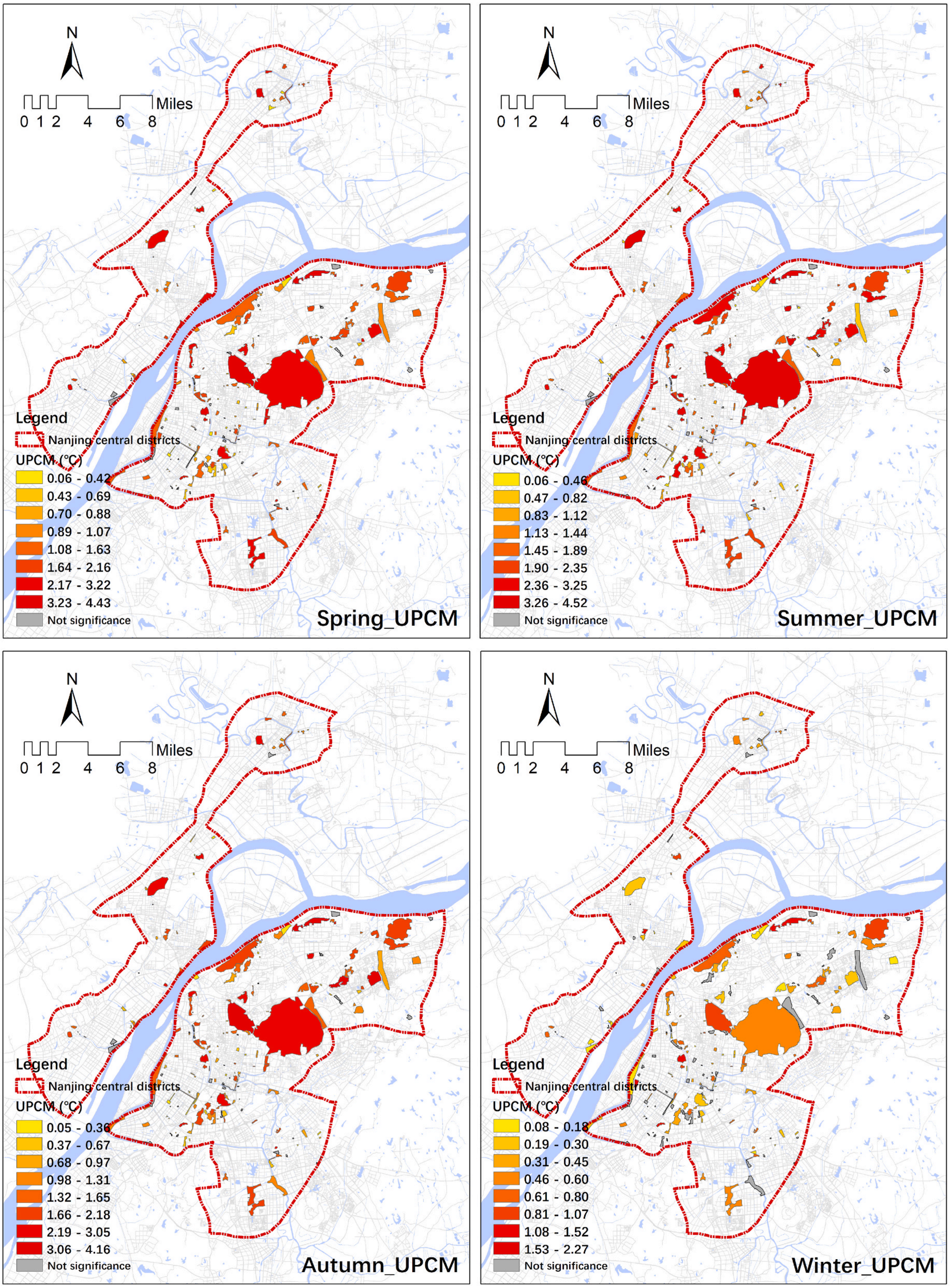

Fig. 6. Distribution of UPCM in four seasons.

P_DYR and B_ABH has largest increase in explanatory power, which could explain almost 89% of UPCM, although its individual cumulation is not significant (22%). In winter, the two-factor q-values are generally lower than in the other three seasons, but the increase percentages are higher, and almost every interaction more than doubles the explanatory power comparing to the individual cumulations in top 10 pairwise interactions.

3.2.3. Dominant factors and their importance to UPCM

Multiple stepwise regression helped us identify the dominant factors of UPCM in the four seasons (Table 5). Among them, the Durbin Watson (DW) statistical test values were all near 2 (acceptable range: 1.7–2.3),

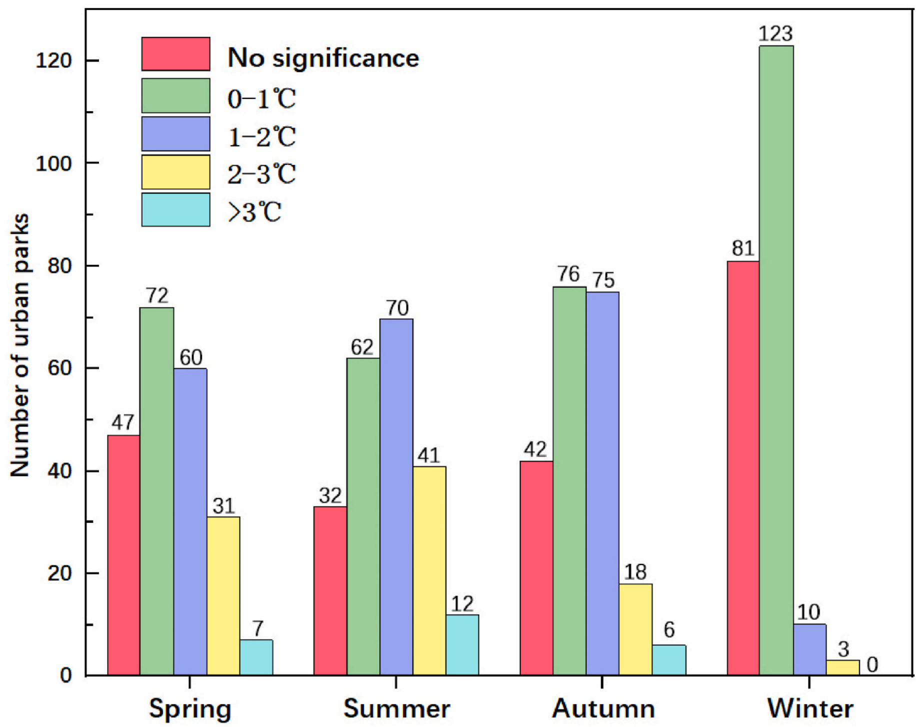

Fig. 7. The number of urban parks with different UPCM.

indicating that the four regression models had no first-order autocorrelation, and the models were well constructed. The R^2 statistic represents the percentage of UPCM explained by the regression model; it explained 55.7%, 53.3%, 62.0%, and 50.5% of the variance of the UPCM in spring, summer, autumn, and winter, respectively. Standardized coefficients indicate the relative importance of factors, and all factors were significant at the 0.005 level ($P < 0.005$). Among the four seasons, NDVI and NDWI were identified as the most important influencing factors of UPCM. In spring and winter, P_NDWI was identified as the most dominant factor affecting UPCM, while P_NDVI was the most important influencing factor in summer and autumn. According to the regression model, in spring, for every 0.1 increase in P_NDWI, the UPCM will increase by 0.5248 °C. In summer, for every 0.1 increase in P_NDVI, the UPCM will increase by 0.5585 °C. In addition, PP will positively affect the UPCM in four seasons, although its importance is relatively low, which means that a park with a larger perimeter will have a better cooling effect on the surrounding environment.

3.2.4. *Factor analysis of under multidimensional indexes*

As shown in Fig. 12, the PA, PP, P_LSI, P_NDVI, PE, and B_NDVI were positively correlated with UP_{MCS} in different seasons, and the PA, PP, P_NDVI, P_NDWI, and B_NDVI were the most significant ($p < 0.001$). B_BD will negatively affect UP_{MCS}, indicating that parks with high surrounding building density have relatively low UP_{MCS}. UP_{MCE} is negatively correlated with PA and PP, which indicates that although a larger park has a larger effective cooling area compared with its own area, the cooling efficiency is relatively low. Thus, small parks are more economical. UP_{MCE} in summer and winter is negatively correlated with P_DCC, which indicates that the closer the park is to the city center, the higher the efficiency of cooling in these two seasons, especially in summer. In addition, in spring and summer, B_BD is positively correlated with UP_{MCE}, indicating that the lower the surrounding building density, the greater the UP_{MCE}. Similarly, in summer, when the average building height around parks is higher, UP_{MCE} is also larger.

UP_{CCI} and UP_{CCG} were weakly correlated with PA. PP, P_NDVI, B_NDVI, and B_NDWI had the most positive effects on UP_{CCI} and UP_{CCG} in spring, summer, and autumn ($p < 0.001$). In winter, UP_{CCI} and UP_{CCG} were positively correlated with P_LSI, P_NDVI, and B_NDVI and negatively correlated with B_ABH and B_BD. In summer and autumn, B_BD significantly negatively affected UP_{CCI}, but in spring and winter, this effect was not significant. UP_{CCG} in summer and autumn was negatively correlated with P_DYR, indicating that the closer the park is to the Yangtze River, the greater the UP_{CCG}. In addition, P_NDVI had significant positive impacts on UP_{CCG} in spring and autumn, but had little impact on UP_{CCG} in other seasons. Correspondingly, B_NDVI had a significant positive effect on UP_{CCG} in all seasons.

4. Discussions

4.1. *Seasonal cooling effects of urban parks and their built environment factors*

Natural interventions, such as urban parks, are effective at mitigating UHIs, since they usually contain vegetation and water [3]. The thermal stability of water and transpiration of plants result in a lower LST inside a park than in the surrounding areas [45,65]. Current studies focus on summer and extreme heat, as urban park cooling tends to perform better in summer than in the other three seasons, which is consistent with our findings [39,66].

Many studies have shown a high correlation between LST and urban thermal comfort [21,22,67]. Identifying the main factors affecting UPSCE will help to improve the surface thermal environment and thermal comfort of urban parks and their surroundings in a specific season. This study is consistent with the basic consensus that PA, PP, P_NDVI, and P_NDWI positively affect UPCE in summer [16,32,36,68]. Multiple stepwise regression analysis showed that P_NDVI and P_NDWI were the dominant factors of UPCM in spring, summer, and autumn. For example, in summer, if P_NDVI and P_NDWI increased by 0.1, the UPCM would increase by 0.5585 °C and 0.3351 °C, respectively. However, the regression model failed to explain about 40–50% of the variability. The possible two reasons are: firstly, this study detected the macro-seasonal impacts of the blue-green index, buildings, and other geographical environments on UPSCE. Micro factors such as vegetation type, building materials and air humidity, which are likely to affect UPSCE, were not

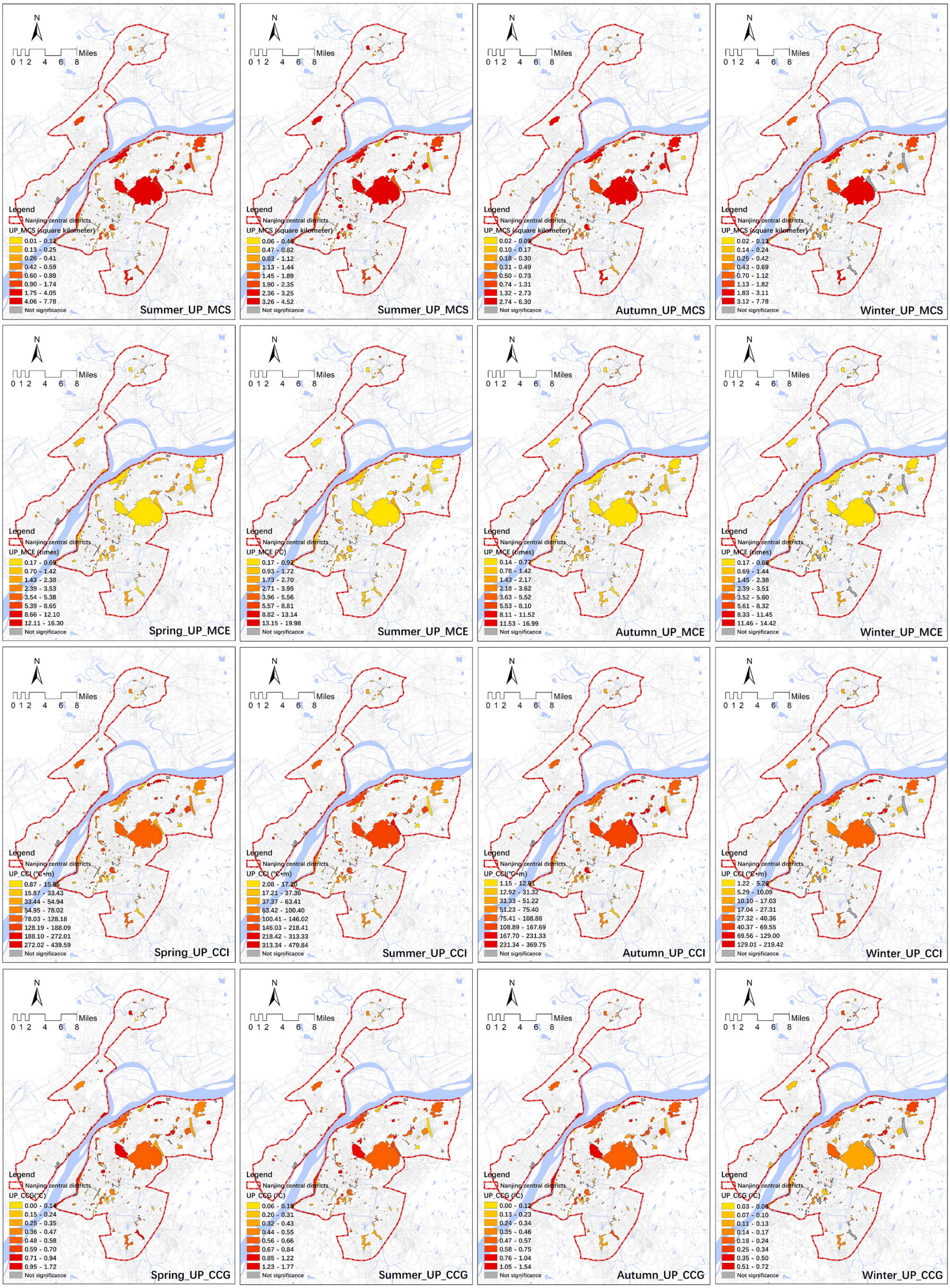

Fig. 8. Distribution of multidimensional indexes of UPSCE.

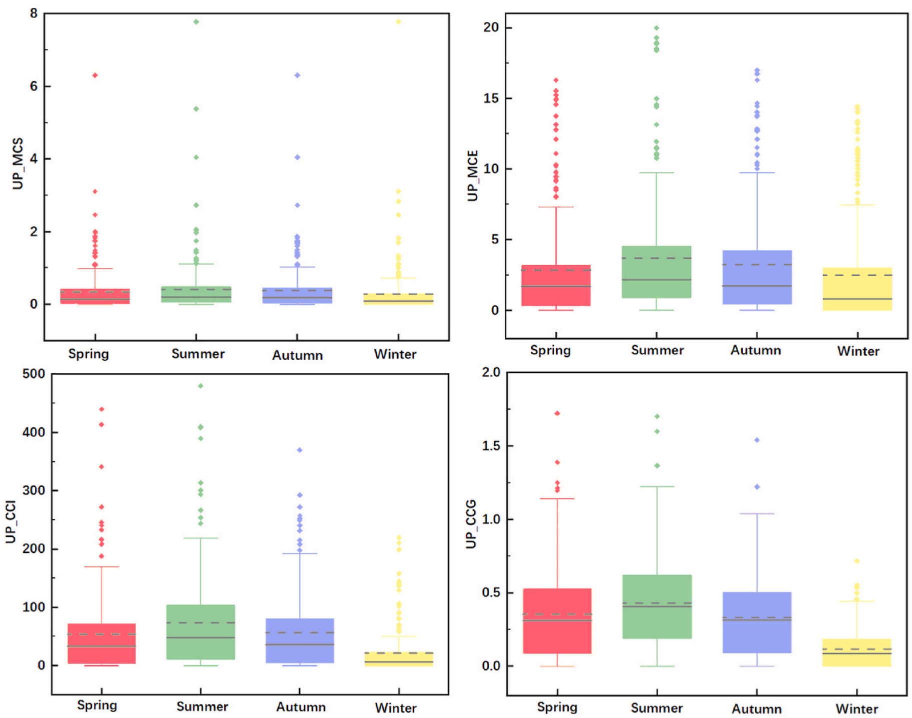

Fig. 9. Boxplot of multidimensional indexes of UPSCE
Note: dotted line: mean; solid line: median.

Table 3
Descriptive statistics of influence factors.

Factors		Number	Mean	Standard deviation	Minimum	Maximum
PA (km^2)		217	0.37	1.90	<0.01	26.82
PP (km)		217	2.14	2.75	0.17	27.27
P_LSI		217	1.49	0.48	1.01	4.64
P_NDVI	Spring	217	0.22	0.08	0.06	0.38
	Summer	217	0.31	0.09	0.10	0.54
	Autumn	217	0.27	0.10	0.07	0.49
	Winter	217	0.12	0.02	0.03	0.18
P_NDWI		217	0.12	0.08	0	0.51
PE (m)		217	20.68	15.78	4.57	99.08
P_DCC (km)		217	6.31	3.99	0.02	18.93
P_DYR (km)		217	0.98	0.72	0.06	3.46
B_NDVI	Spring	217	0.12	0.04	0	0.23
	Summer	217	0.19	0.06	0	0.37
	Autumn	217	0.15	0.09	0	0.34
	Winter	217	0.08	0.02	0	0.13
B_NDWI		217	0.12	0.08	0	0.45
B_ABH (m)		217	24.32	21.43	0	119.54
B_BD		217	0.09	0.08	0	0.61

Table 4
Factor detection of UPCM.

UPCM	X1	X2	X3	X4	X5	X6	X7	X8	X9	X10	X11	X12
Spring	0.36 ***	0.36 ***	0.14	0.19**	0.16*	0.22 ***	0.12	0.13	0.12	0.22***	0.15*	0.14
Rank	1	2	9	5	6	3	11	10	12	4	7	8
Summer	0.40 ***	0.38 ***	0.12	0.36***	0.16*	0.20 ***	0.16 *	0.15 *	0.07	0.29 ***	0.22 ***	0.18 **
Rank	1	2	11	3	9	6	8	10	12	4	5	7
Autumn	0.44 ***	0.40 ***	0.14	0.39***	0.18*	0.11	0.13	0.10	0.10	0.18 **	0.18 **	0.14
Rank	1	2	8	3	5	10	9	11	12	4	6	7
Winter	0.18 *	0.17 *	0.09	0.14	0.19**	0.07	0.16 *	0.09	0.07	0.05	0.08	0.13
Rank	2	3	7	5	1	10	4	8	11	12	9	6

Note: *, **, and *** represent significance at the 0.05, 0.01, and 0.001 levels, respectively.

	X1	X2	X3	X4	X5	X6	X7	X8	X9	X10	X11	X12
X1	0.36	EB	EN	EN	EN	EN	EN	EN	EN	EN	EN	EN
X2	0.56	0.36	EN	EN	EN	EN	EN	EN	EN	EN	EN	EN
X3	0.83	0.87	0.14	EN	EN	EN	EN	EN	EN	EN	EN	EN
X4	0.89	0.81	0.82	0.19	EN	EN	EN	EN	EN	EN	EN	EN
X5	0.85	0.87	0.77	0.70	0.16	EN	EN	EN	EN	EN	EN	EN
X6	0.81	0.83	0.86	0.73	0.82	0.22	EN	EN	EN	EN	EN	EN
X7	0.81	0.87	0.77	0.76	0.84	0.81	0.12	EN	EN	EN	EN	EN
X8	0.85	0.86	0.87	0.85	0.81	0.83	0.80	0.13	EN	EN	EN	EN
X9	0.92	0.83	0.87	0.81	0.90	0.83	0.84	0.86	0.12	EN	EN	EN
X10	0.87	0.91	0.80	0.90	0.81	0.81	0.81	0.75	0.77	0.22	EN	EN
X11	0.76	0.77	0.83	0.70	0.75	0.84	0.84	0.80	0.79	0.86	0.15	EN
X12	0.86	0.81	0.86	0.76	0.78	0.84	0.84	0.76	0.76	0.83	0.76	0.14

(a) Spring

	X1	X2	X3	X4	X5	X6	X7	X8	X9	X10	X11	X12
X1	0.40	EB	EN	EN	EN	EN	EN	EN	EN	EN	EN	EN
X2	0.61	0.38	EN	EN	EN	EN	EN	EN	EN	EN	EN	EN
X3	0.86	0.78	0.12	EN	EN	EN	EN	EN	EN	EN	EN	EN
X4	0.90	0.85	0.89	0.36	EN	EN	EN	EN	EN	EN	EN	EN
X5	0.83	0.86	0.90	0.86	0.16	EN	EN	EN	EN	EN	EN	EN
X6	0.82	0.85	0.85	0.81	0.81	0.20	EN	EN	EN	EN	EN	EN
X7	0.87	0.88	0.85	0.90	0.84	0.69	0.16	EN	EN	EN	EN	EN
X8	0.86	0.90	0.85	0.86	0.78	0.72	0.76	0.15	EN	EN	EN	EN
X9	0.88	0.82	0.82	0.86	0.84	0.80	0.82	0.89	0.07	EN	EN	EN
X10	0.91	0.88	0.70	0.76	0.76	0.66	0.78	0.73	0.77	0.29	EN	EN
X11	0.74	0.76	0.86	0.88	0.88	0.79	0.73	0.82	0.80	0.78	0.22	EN
X12	0.88	0.87	0.87	0.86	0.86	0.83	0.86	0.78	0.86	0.76	0.79	0.18

(b) Summer

	X1	X2	X3	X4	X5	X6	X7	X8	X9	X10	X11	X12
X1	0.44	EB	EN	EN	EN	EN	EN	EN	EN	EN	EN	EN
X2	0.62	0.40	EN	EN	EN	EN	EN	EN	EN	EN	EN	EN
X3	0.87	0.79	0.14	EN	EN	EN	EN	EN	EN	EN	EN	EN
X4	0.91	0.86	0.81	0.39	EN	EN	EN	EN	EN	EN	EN	EN
X5	0.85	0.94	0.90	0.92	0.18	EN	EN	EN	EN	EN	EN	EN
X6	0.87	0.88	0.82	0.76	0.81	0.11	EN	EN	EN	EN	EN	EN
X7	0.88	0.88	0.83	0.83	0.83	0.82	0.13	EN	EN	EN	EN	EN
X8	0.81	0.84	0.80	0.89	0.74	0.74	0.76	0.10	EN	EN	EN	EN
X9	0.89	0.92	0.79	0.83	0.85	0.67	0.83	0.71	0.10	EN	EN	EN
X10	0.93	0.90	0.84	0.85	0.81	0.63	0.84	0.87	0.60	0.18	EN	EN
X11	0.84	0.86	0.82	0.80	0.81	0.85	0.77	0.78	0.78	0.78	0.18	EN
X12	0.93	0.91	0.80	0.89	0.83	0.86	0.82	0.71	0.83	0.81	0.81	0.14

(c) Autumn

	X1	X2	X3	X4	X5	X6	X7	X8	X9	X10	X11	X12
X1	0.18	EB	EN	EN	EN	EN	EN	EN	EN	EN	EN	EN
X2	0.50	0.17	EN	EN	EN	EN	EN	EN	EN	EN	EN	EN
X3	0.69	0.77	0.09	EN	EN	EN	EN	EN	EN	EN	EN	EN
X4	0.67	0.7	0.67	0.14	EN	EN	EN	EN	EN	EN	EN	EN
X5	0.80	0.87	0.78	0.73	0.19	EN	EN	EN	EN	EN	EN	EN
X6	0.66	0.72	0.72	0.64	0.68	0.07	EN	EN	EN	EN	EN	EN
X7	0.79	0.71	0.82	0.7	0.81	0.68	0.16	EN	EN	EN	EN	EN
X8	0.81	0.79	0.71	0.78	0.78	0.61	0.69	0.09	EN	EN	EN	EN
X9	0.80	0.78	0.73	0.76	0.81	0.68	0.8	0.57	0.07	EN	EN	EN
X10	0.82	0.77	0.73	0.72	0.81	0.73	0.78	0.68	0.53	0.05	EN	EN
X11	0.70	0.74	0.67	0.62	0.79	0.63	0.68	0.74	0.69	0.66	0.08	EN
X12	0.75	0.76	0.7	0.8	0.78	0.73	0.72	0.7	0.67	0.75	0.63	0.13

(d) Winter

Fig. 10. Factor interaction detection of UPCM
Note: EN means nonlinear enhancement of two factors; EB means bilinear enhancement of two factors.

Rank	Two-Factor interaction	q(X1)+q(X2)	q(x1∩x2)	Enhancement comparing single-factor
1	PA∩B_ABH	0.48	0.92	91.67%
2	PP∩B_BD	0.58	0.91	56.90%
3	P_NDWI∩B_ABH	0.41	0.90	119.51%
4	P_NDVI∩B_BD	0.28	0.90	221.43%
5	PA∩P_NDVI	0.55	0.89	61.82%
6	PP∩B_BD	0.58	0.87	50.00%
7	PP∩B_NDWI	0.50	0.87	74.00%
8	P_LSI∩P_DYR	0.27	0.87	222.22%
9	PA∩B_BD	0.58	0.87	50.00%
10	PP∩P_NDWI	0.50	0.87	74.00%

(a) Spring

Rank	Two-Factor interaction	q(X1)+q(X2)	q(x1∩x2)	Enhancement comparing single-factor
1	PA∩B_BD	0.69	0.91	31.88%
2	PA∩P_NDVI	0.76	0.90	18.42%
3	P_LSI∩P_NDWI	0.28	0.90	221.43%
4	P_NDVI∩P_DCC	0.52	0.90	73.08%
5	PP∩P_DYR	0.53	0.90	69.81%
6	P_DYR∩B_ABH	0.22	0.89	304.55%
7	PP∩P_DCC	0.54	0.89	64.81%
8	PA∩B_NDWI	0.58	0.88	51.72%
9	P_NDVI∩B_NDWI	0.54	0.88	62.96%
10	P_LSI∩P_NDVI	0.48	0.88	83.33%

(b) Summer

Rank	Two-Factor interaction	q(X1)+q(X2)	q(x1∩x2)	Enhancement comparing single-factor
1	PP∩P_NDWI	0.58	0.94	62.07%
2	PA∩B_NDVI	0.58	0.93	60.34%
3	PA∩B_BD	0.62	0.93	50.00%
4	PP∩B_ABH	0.50	0.92	84.00%
5	P_NDVI∩P_NDWI	0.57	0.92	61.40%
6	PA∩P_NDVI	0.83	0.91	9.64%
7	PP∩B_NDWI	0.54	0.91	68.52%
8	PP∩B_BD	0.58	0.90	55.17%
9	P_LSI∩P_NDWI	0.32	0.90	181.25%
10	P_NDVI∩P_DYR	0.49	0.89	81.63%

(c) Autumn

Rank	Two-Factor interaction	q(X1)+q(X2)	q(x1∩x2)	Enhancement comparing single-factor
1	PP∩P_NDWI	0.25	0.87	248.00%
2	P_LSI∩P_DCC	0.25	0.82	228.00%
3	PA∩B_BD	0.23	0.82	256.52%
4	PA∩P_DYR	0.27	0.81	200.00%
5	P_NDWI∩B_BD	0.24	0.81	237.50%
6	P_NDWI∩B_ABH	0.26	0.81	211.54%
7	P_NDWI∩P_DCC	0.35	0.81	131.43%
8	PA∩P_NDWI	0.37	0.80	116.22%
9	P_DCC∩B_ABH	0.23	0.80	247.83%
10	PA∩B_BD	0.25	0.80	220.00%

(d) Winter

Fig. 11. The 10 pairwise interactions with the largest q value in four seasons.

included. Second, multiple regression is based on linear regression to screen out the factors with the greatest contribution. However, due to the complexity of UPCE, it may be nonlinearly related to the built environment.

The contribution of LSI to UPCE remains uncertain and controversial [38]. Some believe that urban parks with regular and compact shapes tend to have better cooling effects [40,68], while others believe the opposite [41]. This inconsistency might be due to different spatial extents and scales used in the study of UPCE, as suggested by Xiao et al. (2023). This study is consistent with Monteiro et al. (2016). Unlike in other studies, in this study, the PE, P_DYR and P_DCC were included in the factor index system. The PE was shown to be positively correlated with UP_{MCS}, UP_{CCI}, and UP_{CCG} at different confidence levels while significantly driving the UPCM in spring and summer, indicating that mountain parks tend to have better cooling effects than other parks. P_DYR and P_DCC are local factors in Nanjing, China, the former affecting UP_{CCG} in summer and autumn, and the latter driving UPCM and UP_{MCE} in summer, with less impact in other seasons.

We further considered the impacts of a park's surrounding environment on the cooling effects, which has been neglected in many studies [32,68]. Both B_NDVI and B_NDWI affect the cooling effects to varying levels. The results of geographic detectors and Pearson analysis show that park cooling effects are more likely to be driven by B_BD in spring, summer, and autumn than in winter. Han et al. (2023) confirmed that the contributions of B_BD around urban parks to the UPCE are 20.1% and 8.8% in extremely hot weather and normal weather, respectively [35], which is similar to our research. In addition, in summer, the height and density of buildings around parks were shown to positively affect UP_{MCE}. Since city center have higher building density and height, the UP_{MCE} of the park located in the city center can be increased to achieve the best cooling effect.

Table 5
Regression analysis results of UPCM influencing factors.

UPCM	Factor	Unstandardized coefficients		Standardized coefficients	t	p	Tolerance	VIF	R^2	Adjusted R^2	F ($p < 0.001$)	DW
		B	Std.	Beta								
Spring	**Constant**	−1.346	0.181	/	−7.521	0.000	/	/	0.557	0.549	66.748	1.828
	P_NDWI	5.248	0.612	0.453	8.983	0.000	0.822	1.216				
	P_NDVI	3.752	0.552	0.431	8.000	0.000	0.718	1.393				
	B_NDWI	3.419	0.557	0.297	6.350	0.000	0.952	1.050				
	PP	0.100	0.027	0.160	3.071	0.002	0.770	1.299				
Summer	**Constant**	−1.197	0.196	/	−6.103	0.000	/	/	0.533	0.522	59.857	1.743
	P_NDVI	5.585	0.596	0.521	9.377	0.000	0.718	1.393				
	P_NDWI	3.351	0.661	0.263	5.073	0.000	0.822	1.216				
	B_NDWI	3.334	0.601	0.267	5.545	0.000	0.952	1.050				
	PP	0.069	0.020	0.185	3.455	0.004	0.770	1.299				
Autumn	**Constant**	−1.194	0.151	/	−7.888	0.000	/	/	0.620	0.611	68.847	1.911
	B_NDVI	1.978	0.635	0.198	3.114	0.002	0.445	2.249				
	P_NDVI	4.017	0.521	0.465	8.094	0.000	0.546	1.833				
	P_NDWI	3.172	0.504	0.295	6.228	0.000	0.820	1.220				
	B_NDWI	2.178	0.570	0.207	3.820	0.000	0.615	1.625				
	PP	0.049	0.015	0.154	3.174	0.002	0.760	1.316				
Winter	**Constant**	0.111	0.046	/	2.144	0.017	/	/	0.505	0.498	43.361	2.148
	P_NDWI	1.290	0.267	0.313	4.833	0.000	0.994	1.012				
	B_NDVI	1.004	0.154	0.276	3.339	0.000	0.878	1.354				
	PP	0.046	0.010	0.117	3.303	0.008	0.779	1.295				

Note: Regression coefficients include standardized coefficients (Beta) and unstandardized coefficients (B).
Regression models of the four seasons.
Spring _ UPCM = 5.248 P_NDWI +3.752 P_NDVI +3.419 B_NDWI +0.100 PP − 1.346.
Summer _ UPCM = 5.585 P_NDVI +3.351 P_NDWI +3.334 B_NDWI +0.069 PP – 1.197.
Autumn _ UPCM = 1.978 B_NDVI +4.017 P_NDVI +3.172 P_NDWI +2.178 B_NDWI – 0.049 PP – 1.194.
Winter _ UPCM = 1.290 P_NDWI +1.004 B_NDVI +0.046 PP + 0.111.

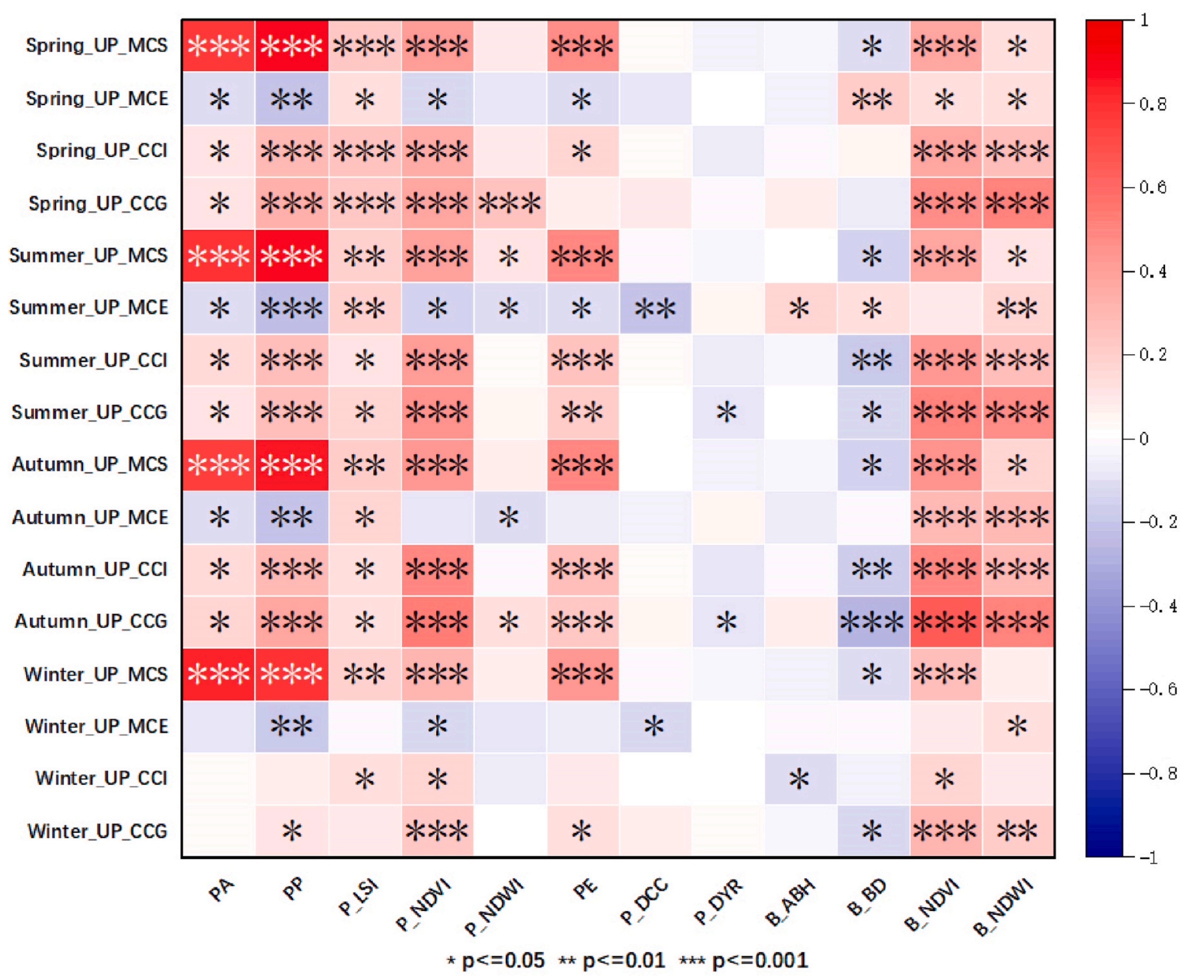

Fig. 12. Pearson analysis of the factors of UPSCE multidimensional indexes.

4.2. Implications for urban park planning and management

Nature-based solutions are receiving increasing attention in the planning and design of urban green space (UGS), which plays an important role in air purification, climate regulation, environmental monitoring, and habitat improvement [69,70]. This study explores the main factors of UPSCE, and their importance, which are important for modulating park cooling effects in specific seasons.

Nanjing, China, has cold summers and hot winters, and the temperature in spring and autumn is relatively suitable; hence, the optimization of urban parks based on cooling effects should focus on summer and winter. In spring, summer, and autumn, the PA and PP had significant effects on urban park cooling. Nevertheless, it is challenging to build parks of sufficient scale in central districts with high construction density and limited land resources [57]. Therefore, it is of paramount importance to achieve optimal cooling effects with the smallest park size [32,33,68]. For example, in spring, summer, and autumn, Nanjing's main city has greater building heights and densities than its surrounding areas, which negatively affects UPCM. Adding small green spaces, such as pocket parks and linear parks, has been shown in many studies to have good UP_{MCE} in densely built-up areas [20,32–34,68]. Parks near the Yangtze River and higher in PE tend to have higher UPCM and UP_{MCS} in hot summer, and these have little influence in other seasons. Therefore, parks can be arranged in areas close to the Yangtze River or be combined with mountains, which can ensure a good landscape and have a good cooling effect in hot summers.

With the rapid urbanization and the shift from urban planning to stock planning, the renewal and optimization of stock parks have become an important part of urban renewal action [20,38]. Although the PA and PP are difficult to expand again, the optimization of stock parks is an effective means to coordinate park cooling effects in different seasons. The P_NDVI was significantly associated with park cooling effects in spring, summer, and autumn, and for every 0.1 increase in PNDVI, the UPCM increased by 0.38 °C, 0.56 °C, and 0.40 °C, respectively. This is higher than the that reported by Xiao et al. (2023) [38], possibly because we used more samples. In early spring, most vegetation is still in the budding stage, and in early autumn, it has just entered the decay stage. Therefore, the mean PNDVI (0.22) in spring is slightly lower than that in autumn (0.27). In winter, the effect of P_NDVI is greatly weakened due to the withered vegetation. Planting an appropriate number of deciduous plants inside the park can reduce the impact on its thermal comfort in winter [68]. In addition, the interaction of factors will enhance the impact on park cooling effects. In summer and autumn, the interaction of P_NDVI and P_NDWI significantly enhanced the explanatory power of UPCM ($q = 0.86$, $q = 0.92$, respectively), which was greater than that in spring ($q = 0.70$) and winter ($q = 0.73$), a finding that has been mentioned but not confirmed in other studies. Therefore, green and blue spaces can be combined to form large blue-green cooling patches by planning a certain area of vegetation around water bodies [13,71]. The seasonal coordination of climate adaptation scenarios can provide new insights into sustainable climate adaptation.

4.3. Limitations and future prospects

Some limitations should be acknowledged. Firstly, the 30 m-resolution LST data used in this study are limited in precision and are more appropriate for macroscopic experiments on an urban or regional scale. Future studies could use higher-resolution images, or use temperature sensing devices, computer parameter simulations (such as ENVI-met), etc. to compare seasonal differences in microclimate regulation of different parks at the microscopic scale [11,18,19]. These methods may also be more effective in exploring the effects of human activities [72], vegetation density and type [73,74], vertical structure [75], and multi-layer flora [73] on UPCE. Secondly, it is challenging to monitor air temperature at an urban scale, so LST is used to measure UPSCE. Although LST has been proven to be highly correlated with thermal comfort in many studies, it can't replace thermal comfort completely. Future studies should not only focus on how much the urban park reduces surface environment temperatures, but also on outdoor thermal comfort indices, such as the Universal Thermal Climate Index (UTCI) [76,77], the Standard Effective Temperature (SET) [78], or Humidex [79], which may provide a better metric for optimizing UPSCE and improving thermal comfort. In addition, we studied only Nanjing, China, as an example for empirical research. Fully understanding the seasonal differences in UPCE in different climate zones will require research in more cities across climate zones, such as cold regions, regions with hot summer and warm winter [34]. Finally, this study only confirmed the individual and interactive effects of the park internal and surrounding built environment on the UPSCE. In the future, it is necessary to further determine the thresholds of UPSCE factors, and achieve the best seasonal coordination through quantitative control.

5. Conclusions

In this study, we investigated the seasonal variations in the cooling effects of 217 urban parks in Nanjing central districts, and identified the individual and interactional impacts of built environment on these variations. A methodological framework is used to compensate for seasonal uncertainty in previous studies. This scheme is suitable for exploring parks to regulate the surface thermal environment or thermal comfort on an urban or larger scale. Our research includes two main conclusions.

(1) Urban parks act as cooling islands to regulate urban microclimate, their cooling to themselves and surroundings will make local areas differ from other urban areas. Contrary to traditional cognition, this study demonstrate that urban parks cooling occurs in any season, not just in the hot seasons. In investigations of 217 parks, the average UPCM in summer reached 1.28 °C, which was higher than that in spring (1.07 °C) and autumn (1.01 °C) and almost four times that in winter (0.30 °C). The average UP_{MCS}, UP_{MCE}, UP_{CCI}, and UP_{CCG} in summer are 0.41 km^2, 3.70 times, 73.70 °C*m, and 0.43 °C, also higher than spring and autumn, much higher than winter. However, although UPCE in winter is not as strong as in other seasons, it is also not negligible. Among them, more than 30 parks have cooled the surface thermal environment by more than 1 °C. They are likely to affect parks' thermal comfort and surrounding areas. In the future, we need to conduct further research on these parks at the micro scale.

(2) The geographical detectors determined the seasonal impacts of built environment and its interactions on UPCE. Factor detector results showed that PA, PP, and P_NDWI had significant driving effects on UPCM in all seasons, while the effect of P_NDVI on UPCM varied seasonally, and the impact of P_NDVI in winter was significantly reduced. The Interaction detector shows that the interaction of any two factors will enhance the UPSCE, except that PA and PP are bilinear enhancements, and the rest are nonlinear enhancements. For example, in summer and autumn, the interaction of P_NDVI and P_NDWI significantly enhanced the explanatory power of UPCM. In winter, the explanatory power of factor interaction is generally weaker than that of other seasons, but the percentage of interaction enhancement is higher than that of other seasons. Multiple stepwise regression showed that the P_NDVI, P_NDWI, B_NDWI, and PP are the dominant factors affecting the UPCM in spring, summer, and autumn. In winter, as vegetation withers, P_NDWI becomes the main factor, which is consistent with the geographic detector results. In addition, we found that under the multidimensional index system, the correlation between factors and UPSCE varies with seasons. For

example, PA, PP, and PE have opposite effects on UP_{MCS} and UP_{MCE}.

Although urban parks can effectively reduce ambient high temperatures, how to maximize the cooling effects in a specific season without compromising the thermal comfort of using park and their surroundings in other seasons remains a challenge. We made suggestions from the aspects of planning layout and stock optimization, including the following: (1) use sporadic plots to increase small green spaces in high-density main cities; (2) lay out parks close to the Yangtze River or combine them with mountains; (3) plant an appropriate number of deciduous plants in parks and their surrounding roads and squares; (4) plant an appropriate number of green plants around water bodies to form blue-green cooling patches. This study provides new insights into more sustainable climate adaptation policies through interventions of planning and design to improve the surface thermal environment and thermal comfort of using park or their surroundings in different seasons.

Role of the funding source

This research was funded by the National Natural Science Foundation of China (No.41001086).

CRediT authorship contribution statement

Zhengyuan Liang: Writing – review & editing, Writing – original draft, Visualization, Software, Methodology, Investigation, Formal analysis, Data curation, Conceptualization. **Zhiming Li:** Writing – review & editing, Writing – original draft, Supervision, Project administration, Methodology, Funding acquisition, Conceptualization. **Zhengxi Fan:** Software, Methodology, Investigation, Formal analysis, Data curation.

Declaration of competing interest

No conflict of interest exists in the submission of this manuscript, and the manuscript is approved by all authors for publication. I would like to declare on behalf of my co-authors that the work described was original research that has not been published previously, and not under consideration for publication elsewhere, in whole or in part. All the authors listed have approved the manuscript that is enclosed.

Data availability

The raw/processed data required to reproduce these findings cannot be shared at this time as the data also forms part of an ongoing study.

References

[1] S. Meerow, L. Keith, Planning for Extreme Heat, A National Survey of U.S. Planners, 2022, p. 88.
[2] Y.L. Li, S.X. Fan, K. Li, Y. Zhang, L.X. Kong, Y.F. Xie, L. Dong, Large Urban Parks Summertime Cool and Wet Island Intensity and its Influencing Factors in Beijing, China, vol. 65, Urban Forestry & Urban Greening, 2021.
[3] K. Kim, C. Yi, S. Lee, Impact of urban characteristics on cooling energy consumption before and after construction of an urban park: the case of Gyeongui line forest in Seoul, Energy Build. 191 (2019) 42–51.
[4] H. Algretawee, S. Rayburg, M. Neave, Estimating the effect of park proximity to the central of melbourne city on urban heat island (UHI) relative to land surface temperature (LST), Ecol. Eng. 138 (2019) 374–390.
[5] F. Ma, X. Yuan, Impact of climate and population changes on the increasing exposure to summertime compound hot extremes, Sci. Total Environ. 772 (2021).
[6] S. Kim, F. Sun, C.I.J.J.o.t.A.P. Association, Planning for climate change: implications of high temperatures and extreme, Heat for Los Angeles County (CA) (4) (2020) 1–11.
[7] C. Tuholske, K. Caylor, C. Funk, A. Verdin, S. Sweeney, K. Grace, P. Peterson, T. Evans, Global urban population exposure to extreme heat (2021) 41.
[8] T.H. Lan, Y.X. Liu, G.L. Huang, J. Corcoran, J. Peng, Urban green space and cooling services: opposing changes of integrated accessibility and social equity along with urbanization, Sustain. Cities Soc. 84 (2022).
[9] S.B. Wu, W.B. Yu, B. Chen, Observed inequality in thermal comfort exposure and its multifaceted associations with greenspace in United States cities, Landsc. Urban Plann. 233 (2023).
[10] H. Yan, F. Wu, L. Dong, Influence of a large urban park on the local urban thermal environment, Sci. Total Environ. 622 (2018) 882–891.
[11] J. Lu, Q.S. Li, L.Y. Zeng, J. Chen, G.X. Liu, Y.C. Li, W.Y. Li, K.L. Huang, A micro-climatic study on cooling effect of an urban park in a hot and humid climate, Sustain. Cities Soc. 32 (2017) 513–522.
[12] Z. Gao, B.F. Zaitchik, Y. Hou, W.P. Chen, Toward park design optimization to mitigate the urban heat Island: assessment of the cooling effect in five US cities, Sustain. Cities Soc. 81 (2022).
[13] Z.W. Yu, G.Y. Yang, S.D. Zuo, G. Jorgensen, M. Koga, H. Vejre, Critical Review on the Cooling Effect of Urban Blue-Green Space: A Threshold-Size Perspective, vol. 49, Urban Forestry & Urban Greening, 2020.
[14] J. Peng, Q. Liu, Z. Xu, D. Lyu, J.J.L. Wu, U. Planning, How to effectively mitigate urban heat island effect? A perspective of waterbody patch size threshold 202 (2020), 103873.
[15] O. Jay, A. Capon, P. Berry, C. Broderick, R. de Dear, G. Havenith, Y. Honda, R. S. Kovats, W. Ma, A. Malik, N.B. Morris, L. Nybo, S.I. Seneviratne, J. Vanos, K. L. Ebi, Reducing the health effects of hot weather and heat extremes: from personal cooling strategies to green cities, Lancet 398 (10301) (2021) 709–724.
[16] W.H. Zhu, J.B. Sun, C.B. Yang, M. Liu, X.L. Xu, C.X. Ji, How to measure the urban park cooling island? A perspective of absolute and relative indicators using remote sensing and buffer analysis, Rem. Sens. 13 (16) (2021).
[17] D.X. Ma, Y.P. Wang, D. Zhou, Z.Z. Zhu, Cooling Effect of the Pocket Park in the Built-Up Block of a City: a Case Study in Xi'an, China, Environmental Science and Pollution Research.
[18] B.S. Lin, C.T. Lin, Preliminary study of the influence of the spatial arrangement of urban parks on local temperature reduction, Urban For. Urban Green. 20 (2016) 348–357.
[19] J.Y. Yang, X.Y. Hu, H.Y. Feng, S. Marvin, Verifying an ENVI-Met Simulation of the Thermal Environment of Yanzhong Square Park in Shanghai, vol. 66, Urban Forestry & Urban Greening, 2021.
[20] J. Peng, Y. Dan, R. Qiao, Y. Liu, J. Dong, J. Wu, How to quantify the cooling effect of urban parks? Linking maximum and accumulation perspectives, Remote Sens. Environ. 252 (2021).
[21] X.R. Zheng, N. Zhang, X. Wang, Development of a modified thermal humidity index and its application to human thermal comfort of urban vegetation patches, Ecosys. Health Sustain. 8 (1) (2022).
[22] B. Mashhoodi, Environmental justice and surface temperature: income, ethnic, gender, and age inequalities, Sustain. Cities Soc. 68 (2021).
[23] R. Goldblatt, A. Addas, D. Crull, A. Maghrabi, G.G. Levin, S. Rubinyi, Remotely sensed derived land surface temperature (LST) as a proxy for air temperature and thermal comfort at a small geographical scale, Land 10 (4) (2021).
[24] Q. Wang, X.A. Wang, Y. Meng, Y. Zhou, H.T. Wang, Exploring the impact of urban features on the spatial variation of land surface temperature within the diurnal cycle, Sustain. Cities Soc. 91 (2023).
[25] L. Yan, W.X. Jia, S.Q. Zhao, The cooling effect of urban green spaces in metacities: a case study of beijing, China's capital, Rem. Sens. 13 (22) (2021).
[26] M. Markovic, J. Cheema, A. Teofilovic, S. Cepic, Z. Popovic, J. Tomicevic-Dubljevic, M. Pause, Monitoring of spatiotemporal change of green spaces in relation to the land surface temperature: a case study of belgrade, Serbia, Rem. Sens. 13 (19) (2021).
[27] X. Cao, A. Onishi, J. Chen, H. Imura, Quantifying the cool island intensity of urban parks using ASTER and IKONOS data, Landsc. Urban Plann. 96 (4) (2010) 224–231.
[28] W. Liao, Z.W. Cai, Y. Feng, D.X. Gan, X.M. Li, A Simple and Easy Method to Quantify the Cool Island Intensity of Urban Greenspace, vol. 62, Urban Forestry & Urban Greening, 2021.
[29] B. Zhou, D. Rybski, J.P. Kropp, On the statistics of urban heat island intensity, Geophys. Res. Lett. 40 (20) (2013) 5486–5491.
[30] C.R. Chang, M.H. Li, S.D. Chang, A preliminary study on the local cool-island intensity of Taipei city parks, Landsc. Urban Plann. 80 (4) (2007) 386–395.
[31] M.H. Tan, X.B. Li, Quantifying the effects of settlement size on urban heat islands in fairly uniform geographic areas, Habitat Int. 49 (2015) 100–106.
[32] J. Peng, Y.Z. Dan, R.L. Qiao, Y.X. Liu, J.Q. Dong, J.S. Wu, How to quantify the cooling effect of urban parks? Linking maximum and accumulation perspectives, Remote Sens. Environ. 252 (2021).
[33] X. Yao, K.Y. Yu, X.J. Zeng, Y.B. Lin, B.J. Ye, X.B. Shen, J. Liu, How can urban parks be planned to mitigate urban heat island effect in "Furnace cities" ? An accumulation perspective, J. Clean. Prod. 330 (2022).
[34] Y. Zhou, H.L. Zhao, S.C. Mao, G.L. Zhang, Y.L. Jin, Y.C. Luo, W. Huo, Z.H. Pan, P. L. An, F. Lun, Studies on urban park cooling effects and their driving factors in China: considering 276 cities under different climate zones, Build. Environ. 222 (2022).
[35] D.R. Han, X.L. Xu, Z. Qiao, F. Wang, H.Y. Cai, H.M. An, K. Jia, Y.H. Liu, Z.Y. Sun, S. H. Wang, W. Han, The roles of surrounding 2D/3D landscapes in park cooling effect: analysis from extreme hot and normal weather perspectives, Build. Environ. 231 (2023).
[36] J. Blachowski, M. Hajnrych, Assessing the cooling effect of four urban parks of different sizes in a temperate continental climate zone: wroclaw (Poland), Forests 12 (8) (2021).
[37] X.L. Geng, Z.W. Yu, D. Zhang, C.W. Li, Y. Yuan, X.R. Wang, The influence of local background climate on the dominant factors and threshold-size of the cooling effect of urban parks, Sci. Total Environ. 823 (2022).

[38] Y. Xiao, Y. Piao, C. Pan, D.K. Lee, B. Zhao, Using Buffer Analysis to Determine Urban Park Cooling Intensity: Five Estimation Methods for Nanjing, China, vol. 868, Science of the Total Environment, 2023.
[39] G.L. Feyisa, K. Dons, H. Meilby, Efficiency of parks in mitigating urban heat island effect: an example from Addis Ababa, Landsc. Urban Plann. 123 (2014) 87–95.
[40] M. Masoudi, P.Y. Tan, Multi-year comparison of the effects of spatial pattern of urban green spaces on urban land surface temperature, Landsc. Urban Plann. 184 (2019) 44–58.
[41] M.V. Monteiro, K.J. Doick, P. Handley, A. Peace, The impact of greenspace size on the extent of local nocturnal air temperature cooling in London, Urban For. Urban Green. 16 (2016) 160–169.
[42] X.L. Xu, H.Y. Cai, Z. Qiao, L. Wang, C. Jin, Y.N. Ge, L.Y. Wang, F.J. Xu, Impacts of park landscape structure on thermal environment using QuickBird and Landsat images, Chin. Geogr. Sci. 27 (5) (2017) 818–826.
[43] B. Li, X.M. Shi, H.Y. Wang, M.Z. Qin, Analysis of the relationship between urban landscape patterns and thermal environment: a case study of Zhengzhou City, China, Environ. Monit. Assess. 192 (8) (2020).
[44] H.Y. Fan, Z.W. Yu, G.Y. Yang, T.Y. Liu, T.Y. Liu, C.H. Hung, H. Vejre, How to cool hot-humid (Asian) cities with urban trees? An optimal landscape size perspective, Agric. For. Meteorol. 265 (2019) 338–348.
[45] K.B. Qiu, B.Q. Jia, The roles of landscape both inside the park and the surroundings in park cooling effect, Sustain. Cities Soc. 52 (2020).
[46] F.H. Kong, H.W. Yin, C.Z. Wang, G. Cavan, P. James, A satellite image-based analysis of factors contributing to the green-space cool island intensity on a city scale, Urban For. Urban Green. 13 (4) (2014) 846–853.
[47] Z. Yin, Y.X. Zhang, R. Zhang, G.J. Chen, Y.P. Cong, K.M. Ma, Structure of an Urban Green Space Indirectly Affects the Distribution of Airborne Particulate Matter: A Study Based on Structural Equation Modelling, vol. 72, Urban Forestry & Urban Greening, 2022.
[48] M. Das, A. Das, S. Momin, Quantifying the cooling effect of urban green space: a case from urban parks in a tropical mega metropolitan area (India), Sustain. Cities Soc. 87 (2022).
[49] J.F. Wang, X.H. Li, G. Christakos, Y.L. Liao, T. Zhang, X. Gu, X.Y. Zheng, Geographical detectors-based health risk assessment and its application in the neural tube defects study of the heshun region, China, Int. J. Geogr. Inf. Sci. 24 (1) (2010) 107–127.
[50] W. Li, J. Chen, W.K. Chen, Analysis with Geographical Detector on the Influencing Factor of Earthquake Mortality in China, 5th Symposium of Risk Analysis and Risk Management in Western China (WRARM), 2017, pp. 40–45. Guiyang, PEOPLES R CHINA.
[51] X.M. Deng, X.H. Liao, C.C. Xu, H.Y. Yue, Ieee, Analysis of ecological factors affecting beijing city based on geographical detector, in: IEEE International Geoscience and Remote Sensing Symposium (IGARSS), JAPAN, Yokohama, 2019, pp. 7498–7501.
[52] Ministry of Construction of the People's Republic of China, Building Climate Zoning Standard (GB 50178-93), 1994. Retrieved from, http://www.biaozhun8.cn/biaozhun98028/.
[53] G.Y. Yang, Z.W. Yu, G. Jorgensen, H. Vejre, How can urban blue-green space be planned for climate adaption in high-latitude cities? A seasonal perspective, Sustainable Cities and Society 53 (2020).
[54] Nanjing natural resources and planning Bureau, nanjing master planning (2011-2020), Retrieved from, http://ghj.nanjing.gov.cn/ghbz/ztgh/201705/t20170509_874089.html, 2017.
[55] Nanjing green and garden Bureau , nanjing green space system planning (2013-2020), Retrieved from, http://ylj.nanjing.gov.cn/njslhylj/202006/t20200622_1961650.html, 2019.
[56] M.A. Ruiz, M.F. Colli, C.F. Martinez, E.N. Correa-Cantaloube, Park cool island and built environment. A ten-year evaluation in Parque Central, Mendoza-Argentina, Sustain. Cities Soc. 79 (2022).
[57] W. Liao, J.M. Guldmann, L. Hu, Q.W. Cao, D.X. Gan, X.M. Li, Linking urban park cool island effects to the landscape patterns inside and outside the park: a simultaneous equation modeling approach, Landsc. Urban Plann. 232 (2023).
[58] I. Dronova, M. Friedman, I. McRae, F.H. Kong, H.W. Yin, Spatio-temporal non-uniformity of urban park greenness and thermal characteristics in a semi-arid region, Urban For. Urban Green. 34 (2018) 44–54.
[59] L.L. Lu, P. Fu, A. Dewan, Q.T. Li, Contrasting determinants of land surface temperature in three megacities: implications to cool tropical metropolitan regions, Sustain. Cities Soc. 92 (2023).
[60] X.T. Chen, Z.T. Wang, Y. Bao, Q.Y. Luo, W.F. Wei, Combined impacts of buildings and urban remnant mountains on thermal environment in multi-mountainous city, Sustain. Cities Soc. 87 (2022).
[61] P.Y. Lin, S.S.Y. Lau, H. Qin, Z.H. Gou, Effects of urban planning indicators on urban heat island: a case study of pocket parks in high-rise high-density environment, Landsc. Urban Plann. 168 (2017) 48–60.
[62] Q. Zhang, D. Zhou, D. Xu, A. Rogora, Correlation between cooling effect of green space and surrounding urban spatial form: evidence from 36 urban green spaces, Build. Environ. 222 (2022).
[63] J.F. Wang, Y. Hu, Environmental health risk detection with GeogDetector, Environ. Model. Software 33 (2012) 114–115.
[64] Y.Z. Song, J.F. Wang, Y. Ge, C.D. Xu, An optimal parameters-based geographical detector model enhances geographic characteristics of explanatory variables for spatial heterogeneity analysis: cases with different types of spatial data, GIScience Remote Sens. 57 (5) (2020) 593–610.
[65] A. Motazedian, A.M. Coutts, N.J. Tapper, The Microclimatic Interaction of a Small Urban Park in Central Melbourne with its Surrounding Urban Environment during Heat Events, vol. 52, Urban Forestry & Urban Greening, 2020.
[66] Y. Chen, J. Yang, W.B. Yu, J.Y. Ren, X.M. Xiao, J.C. Xia, Relationship between urban spatial form and seasonal land surface temperature under different grid scales, Sustain. Cities Soc. 89 (2023).
[67] A.R. dos Santos, F.S. de Oliveira, A.G. da Silva, J.M. Gleriani, W. Goncalves, G. L. Moreira, F.G. Silva, E.R.F. Branco, M.M. Moura, R.G. da Silva, R.S. Juvanhol, K. B. de Souza, C. Ribeiro, V.T. de Queiroz, A.V. Costa, A.S. Lorenzon, G. F. Domingues, G.E. Marcatti, N.L.M. de Castro, R.T. Resende, D.E. Gonzales, L.A. D. Telles, T.R. Teixeira, G. dos Santos, P.H.S. Mota, Spatial and temporal distribution of urban heat islands, Sci. Total Environ. 605 (2017) 946–956.
[68] C.L. Du, W.X. Jia, M. Chen, L. Yan, K. Wang, How can urban parks be planned to maximize cooling effect in hot extremes? Linking maximum and accumulative perspectives, J. Environ. Manag. 317 (2022).
[69] H.Y. Du, Y.L. Cai, F.Q. Zhou, H. Jian, W.Y. Jiang, Y.Q. Xu, Urban blue-green space planning based on thermal environment simulation: a case study of Shanghai, China, Ecol. Indicat. 106 (2019).
[70] Z.M. Li, Z.Y. Liang, L.H. Feng, Z.X. Fan, Beyond accessibility: a multidimensional evaluation of urban park equity in yangzhou, China, ISPRS Int. J. Geo-Inf. 11 (8) (2022).
[71] W. Zhou, W. Cao, T. Wu, T. Zhang, The win-win interaction between integrated blue and green space on urban cooling, Sci. Total Environ. 863 (2023).
[72] H.Q. Qin, X.X. Cheng, G.F. Han, Y.X. Wang, J.F. Deng, Y.C.A. Yang, How Thermal Conditions Affect the Spatial-Temporal Distribution of Visitors in Urban Parks: A Case Study in Chongqing, China, vol. 66, Urban Forestry & Urban Greening, 2021.
[73] J.X. Wei, H.B. Li, Y.C. Wang, X.Z. Xu, The cooling and humidifying effects and the thresholds of plant community structure parameters in urban aggregated green infrastructure, Forests 12 (2) (2021).
[74] S. Sodoudi, H.W. Zhang, X.L. Chi, F. Muller, H.D. Li, The influence of spatial configuration of green areas on microclimate and thermal comfort, Urban For. Urban Green. 34 (2018) 85–96.
[75] H. Sugawara, K. Narita, T. Mikami, Vertical structure of the cool island in a large urban park, Urban Clim. 35 (2021).
[76] J.S. Wu, C. Liu, H.L. Wang, Analysis of Spatio-temporal patterns and related factors of thermal comfort in subtropical coastal cities based on local climate zones, Build. Environ. 207 (2022).
[77] M. Das, A. Das, Exploring the pattern of outdoor thermal comfort (OTC) in a tropical planning region of eastern India during summer, Urban Clim. 34 (2020).
[78] S. Zhang, Z. Lin, Predicted Mean Vote with skin temperature from standard effective temperature model, Build. Environ. 183 (2020).
[79] G.F. Ghalhari, H. Heidari, S.F. Dehghan, M. Asghari, Consistency assessment between summer simmer index and other heat stress indices (WBGT and Humidex) in Iran's climates, Urban Clim. 43 (2022).